REVIEW

Spectroscopic studies of protein folding: Linear and nonlinear methods

Arnaldo L. Serrano, Matthias M. Waegele, and Feng Gai*

Department of Chemistry, University of Pennsylvania, Philadelphia, Pennsylvania 19104

Received 24 October 2011; Accepted 15 November 2011
DOI: 10.1002/pro.2006
Published online 22 November 2011 proteinscience.org

Abstract: Although protein folding is a simple outcome of the underlying thermodynamics, arriving at a quantitative and predictive understanding of how proteins fold nevertheless poses huge challenges. Therefore, both advanced experimental and computational methods are continuously being developed and refined to probe and reveal the atomistic details of protein folding dynamics and mechanisms. Herein, we provide a concise review of recent developments in spectroscopic studies of protein folding, with a focus on new triggering and probing methods. In particular, we describe several laser-based techniques for triggering protein folding/unfolding on the picosecond and/or nanosecond timescales and various linear and nonlinear spectroscopic techniques for interrogating protein conformations, conformational transitions, and dynamics.

Keywords: 2D-IR; conformational trigger; conformational probe; FCS; fluorescence; FRET; infrared; isotope editing; kinetics; protein folding; Raman; temperature-jump

Introduction

Despite extensive study over the past few decades, the protein folding problem[1] continues to inspire new research directions. This is due not only to the sheer complexity of the process of protein folding, which makes it extremely difficult to achieve a mechanistic, quantitative, and predictive understanding of how proteins fold, but also to the fact that it provides an excellent test-bed for the development and validation of new computational and experimental methods for biology, biochemistry, and biophysics. Herein, we present a concise review of recent advances in the application of spectroscopic methods to investigations of protein folding, with a focus on fluorescence and vibrational spectroscopies, as well as conformational triggering methods. Although dynamic information can sometimes be revealed or inferred by static spectroscopic measurements, for most ensemble kinetic experiments, a suitable triggering event is required to start the "reaction" of interest; in addition, one or more physical observables or probes are used to follow the progression of this reaction. For protein folding studies, it is apparent that the choice of the triggering method determines the time resolution of the observable kinetics, whereas the conformational probes used dictate the structural resolution of the experiment. Below, we will first discuss available protein folding and conformational triggering methods, with a focus on those that offer nanosecond or faster time resolutions, and then will review spectroscopic methods that offer varying degrees of structural resolution and sensitivity when applied to probe protein folding/unfolding equilibria and kinetics.

*Correspondence to: Feng Gai, Department of Chemistry, University of Pennsylvania, Philadelphia, PA 19104.
E-mail: gai@sas.upenn.edu.

Grant sponsor: National Institutes of Health; Grant numbers: GM-065978, RR01348.

Triggering Methods

The free energy of a given protein in solution depends on the temperature, pressure, solvent composition, and other external constraints if they exist. Thus, the thermodynamic equilibrium between its folded and unfolded states can be manipulated by simply changing one of these factors. As such, all current protein folding triggering methods rely on this principle, whereby the system in question is rapidly (compared with the kinetic events of interest) shifted to a nonequilibrium state. The subsequent relaxation kinetics towards the new thermodynamic equilibrium, which could be probed by a wide variety of techniques, can be dominated by either folding, unfolding, or both, depending on the final condition of the protein solution. For example, a folding or unfolding process could be initiated by rapid mixing of two solutions via either the stopped-flow or continuous-flow techniques.[2,3] Although the majority of previous folding kinetic studies used such mixing-based triggering methods, a comprehensive review of these subjects is beyond the scope of this paper. Below we only discuss triggering methods that rely on the application of short (picosecond–nanosecond) laser pulses, which may involve direct excitation of chemical groups in the protein, resulting in chemical changes that leave the protein backbone in a nonequilibrium state (e.g., by removal of a conformational constraint), or photoinduced changes of physical and/or solution properties (e.g., temperature or pH) via excitation of solvent or solute molecules.

Laser-induced temperature-jump

The ultrafast (picosecond or nanosecond) temperature-jump (*T*-jump) method relies on the fact that in condensed phases vibrational relaxations typically take place on the picosecond timescale,[4] thus allowing a burst of photons to rapidly heat up the solution of interest through excitation of solvent or solute[5,6] vibrations. For aqueous solutions, a rapid *T*-jump can be achieved by exciting water's near-infrared (IR) overtone transitions in the vicinity of either 1.5 μm (for H_2O solution) or 2 μm (for D_2O solution) using either nanosecond (ns) or picosecond (ps) laser pulses.[7–12] The amplitude of the *T*-jump depends on the pump energy and excitation volume and can be determined from solvent absorbance using a calibration curve.[7] Because the thermal energy initially concentrated in the laser excitation volume will gradually dissipate into the surroundings, the useful time window of this technique in which the temperature remains approximately constant ranges from a few to tens of milliseconds (ms), depending on the optical setup and sample holder. Because the *T*-jump technique does not require any specific protein modifications, it is, therefore, the most commonly used triggering method in the study of ultrafast protein folding events.[13–23]

Azobenzene isomerization

The reversible cis/trans photoisomerization of azobenzenes has also been demonstrated to have the capability to control peptide and protein conformations and thus has found utility in folding kinetic studies.[24–29] A thorough review on the use of azobenzene and derivatives as photoswitches in biomolecules can be found elsewhere.[30] Simple azobenzene compounds photoisomerize on the ps timescale and, therefore are suitable for studying the early events in protein folding. Additionally the azobenzene cis/trans isomers exhibit well separated spectral features, allowing for independent excitation of either isomer and thus reversible switching of the trigger. As shown first by Kumita *et al.*,[26] a reversible change in helicity of up to 36% can be obtained on photoisomerization of the azobenzene cross-linker in an alanine-based peptide. More recent work has been done to understand how such linkers affect peptide backbone conformations,[31,32] and to probe the dynamics and mechanism of the helix–coil transition,[33–35] among other applications.[36–38]

Photodissociation of a cage compound or disulfide bond

Another method of conformational switching is to use a relatively large molecular moiety (i.e., a cage) to force the protein of interest to unfold under native conditions; on cleavage of the cage by excitation with an appropriate laser pulse, the protein will fold to its native conformation. Thus, several photocages, such as benzoinyl cages, have been used to trigger protein folding kinetics.[39–43] Photocaged molecules can also be used in a cyclization scheme to produce a photocleavable intramolecular linker. In some cases, it is desirable to impose a well defined structural constraint on the protein molecule, enabling the folding/unfolding reaction to start from a unique position on the folding energy landscape on removal of the conformational constraint. For example, this approach has been applied to the study of a mutant of the small α-helical villin headpiece subdomain (i.e., cVHP-34 M12C), in which an internal cysteine residue and a 3′-(carboxymethoxy)benzoin (CMB) molecule, which is covalently attached to the N-terminus of the polypeptide, have been linked to restrict the conformation in the unfolded state. On illumination with a 355 nm laser pulse, this linker molecule is irreversibly cleaved with a yield of 0.6–0.7; the loop is therefore broken to yield the linear protein that is free to refold. The time resolution of this method is determined by the rate of photolysis of the linker, which is faster than one nanosecond.[44] However, it is worth mentioning that if the photocage has to diffuse out of its initial position for the protein to fold, the time resolution of such cage cleaving methods would be determined by the rate of this diffusion process.

One convenient structural constraint commonly found in proteins is the disulfide bond formed between two thiol-containing amino acid sidechains. Lu *et al.*[45] have shown that a disulfide cross-linker can be transiently broken by an ultraviolet (UV) laser pulse, making it potentially useful as a phototriggering method in protein folding studies. However, in practice this method is less useful as the resultant thiyl radicals undergo rapid geminate recombination, which greatly reduces the population of protein molecules that will eventually undergo a conformational transition. Recently, Hamm and coworkers[46,47] have shown that for small peptides this problem can be alleviated to some extent due to the increased strain exerted on the disulfide bond by cross-linking two cysteines that are close in sequence. A more promising method, which is currently under investigation in our laboratory,[48] however, is to use a photoinduced electron transfer (PET) reaction to permanently break the disulfide cross-linker of interest. Cleavage of disulfide bonds via light-induced electron transfer from adjacent tryptophan residues has been observed in various proteins[49–54] suggesting that it could be engineered to control protein/peptide conformations using light.

Other phototriggering methods

Besides the methods discussed above, other avenues for generating high free energy conformations in proteins, such as electron transfer[55,56] and ligand dissociation,[57,58] have also found important applications, some of which have been thoroughly reviewed in the past.[59,60] More recently, Tucker *et al.*[61] have shown that disulfonyl-tetrazine could be used as an ultrafast phototrigger of protein conformations because its photodissociation, which yields N_2, occurs on the ps timescale with a reasonably high yield.

Probing Methods

The greatest challenge in the study of the molecular mechanism of protein folding is that none of the existing experimental techniques are capable of capturing conformational snapshots of the protein in question along its "folding coordinate" with both high spatial and temporal resolutions. As such, a wide variety of spectroscopic techniques have been developed and used, some of which are continuously being refined, to probe the fine detail of certain regions or features of the underlying folding free energy landscape. Although all of these techniques are worthy of discussion, below we will focus on linear and nonlinear methods based on the application of fluorescence and vibrational spectroscopies. The spectroscopic properties of a particular sample are determined by its polarization, $\vec{P}(t)$, induced by the electric field of an incoming light beam, $\vec{E}(t)$, which can be expressed as,[62]

$$\vec{P}(t) = \int_{-\infty}^{t} dt_1 \hat{R}^{(1)}(t_1)\vec{E}(t-t_1) + \sum_{n=2}^{\infty} \int_{-\infty}^{t} dt_n \cdots \times \int_{-\infty}^{t_2} dt_1 \hat{R}^{(n)}(t_n,\cdots,t_1)\vec{E}(t-t_1)\cdots\vec{E}(t-t_n\cdots-t_1) \quad (1)$$

where $\hat{R}^{(n)}(\cdots)$ is the nth order response function of the system. If the electric field is sufficiently weak so that only the first term (i.e., $\hat{R}^{(1)}(t_1)$) in Eq. (1) needs to be considered to describe the underlying light-matter interaction, various linear spectroscopies, such as absorption spectroscopy and fluorescence excitation, result. In contrast, nonlinear spectroscopic techniques require consideration of higher order terms (i.e., $n > 1$) and typically involve application of ultrafast laser pulses.

Native fluorescence

Three aromatic amino acids, that is, tryptophan (Trp), tyrosine (Tyr), and phenylalanine (Phe), are fluorescent and thus could be used to probe protein conformational changes. In practice, however, only Trp fluorescence is extensively used in protein folding studies due to its sensitivity to the environment and its larger quantum yield. Because many reviews[63–67] on Trp fluorescence and its application to protein conformational and folding studies exist in the literature, below we focus the remainder of our discussion on fluorescent methods utilizing nonnative fluorophores.

Nonnative fluorescence

Recently, we have shown that the unnatural amino acid, *p*-cyanophenylalanine (Phe_{CN}), is a very useful fluorescent probe of protein folding and binding.[68] The absorption spectrum of Phe_{CN} exhibits two broad bands, one centered around 240 nm and the other one centered around 280 nm, whereas its fluorescence spectrum peaks at ~295 nm and is insensitive to excitation wavelength and solvent.[69] However, the fluorescence quantum yield (Q_F) of Phe_{CN} is sensitive to its immediate environment (e.g., in water $Q_F = 0.11$, whereas in acetonitrile $Q_F = 0.03$), making it an ideal fluorescent probe of protein folding and binding transitions.[70,71] For example, using this probe, Tang *et al.*[72] have investigated the binding/insertion/dimerization kinetics of a transmembrane peptide. As shown (Fig. 1), their results showed that when placed at the same position Phe_{CN} is a more sensitive fluorescent reporter of the insertion and dimerization processes than Trp.

Moreover, Serrano *et al.*[69] have shown that the fluorescence of Phe_{CN} exhibits single-exponential decay kinetics with a lifetime (τ_F) of 5–8 ns, depending on the solvent. In particular, they found that for a series of protic solvents τ_F increases with increasing hydrogen bonding strength of the solvent, due to

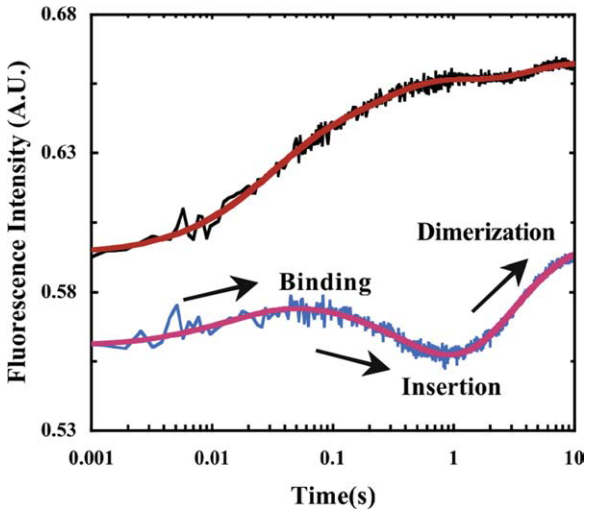

Figure 1. Stopped-flow kinetics of a transmembrane peptide on association with a model membrane probed via Trp (black) and Phe_{CN} (blue) fluorescence, with the latter exhibiting greater sensitivity to the key kinetic events. (Adapted from Tang J, et al., (2009) J Am Chem Soc 131:3816–3817, with permission from American Chemical Society.)[72]

a decrease in the nonradiative rate of the excited state. These findings further indicate that when combined with time-resolved lifetime measurements (see below), Phe_{CN} fluorescence could be used to probe the conformational distribution of proteins under native or nonnative conditions.

Fluorescence resonance energy transfer

Modulation of the fluorescence intensity of a fluorophore of interest by another molecular moiety (or quencher) through various mechanisms[73] has been widely used as a means to measure the proximity of the fluorophore to the quencher. For protein molecules, such modulations have been used to report on conformations and conformational changes as a function of various physical variables (e.g., time, temperature, or denaturant concentration). When fluorescence quenching arises solely from fluorescence resonance energy transfer (FRET), distance information may be obtained. According to Förster theory,[74] the mean FRET efficiency of a fluctuating biopolymer, $\langle E \rangle$, can be expressed as:

$$\langle E \rangle = 1 - \left\langle \frac{r^6}{r^6 + R_0^6} \right\rangle = 1 - \int_0^\infty \frac{r^6}{r^6 + R_0^6} P(r) dr \qquad (2)$$

where r is the separation distance between the donor and acceptor, $P(r)$ is the equilibrium distribution function of the donor–acceptor separation distances, and R_0 is the Förster radius[75] defined as:

$$R_0^6 = \frac{9000 \ln(10) \kappa^2 J Q_D}{128 \pi^5 \eta^4 N_A} \qquad (3)$$

where N_A, η, and Q_D are the Avogadro constant, the refractive index of the solvent, the quantum yield of the donor, respectively, whereas κ describes the relative orientation between the transition dipole moments of the donor and acceptor. J is the overlap integral of the donor fluorescence spectrum and acceptor absorption spectrum.

FRET measurements can be used to determine folding/unfolding thermodynamics. For example, for a simple two-state system, it can be easily shown that the mean energy transfer efficiency as a function of a denaturation variable, x (e.g., temperature, urea concentration, etc.), is

$$\langle E \rangle(x) = \frac{\langle E_f \rangle(x) K_{eq} + \langle E_u \rangle(x)}{1 + K_{eq}} \qquad (4)$$

where $\langle E_f \rangle(x)$ and $\langle E_u \rangle(x)$ are the denaturant dependent transfer efficiency for the folded and unfolded state, respectively, and K_{eq} is the equilibrium constant for unfolding. However, in practice caution must be taken when applying FRET to extract any quantitative information from the experimental data as the R_0 of the FRET pair used may show a strong dependence on x and, in many cases, the accurate determination of is rather difficult.[76]

Recently, we suggested a simpler approach[77] to determine folding/unfolding thermodynamics from FRET denaturation data based on the ratio of the integrated areas of the donor and acceptor fluorescence spectra in the case where the donor quantum efficiency is invariant as a function of unfolding, that is,

$$\frac{F_{DA}}{F_{AD}} = \frac{Q_D \left(\frac{r_f^6}{r_f^6 + R_0^6} + K_{eq} \int_0^\infty \frac{r_6}{r^6 + R_0^6} P_u(r) dr \right)}{Q_{A,f} \frac{R_0^6}{r_f^6 + R_0^6} + K_{eq} Q_{A,u} \left[1 - \int_0^\infty \frac{r^6}{r_6 + R_0^6} P_u(r) dr \right]} \qquad (5)$$

where r is the donor-to-acceptor separation distance, Q_D is the quantum efficiency of the donor, and $Q_{A,f}$ and $Q_{A,u}$ are the quantum efficiencies of the acceptor in the folded and unfolded states, respectively. The above expression can be further simplified if it is assumed that $P(r) = \delta(r)$ holds for both the folded and unfolded state ensembles, yielding two distance parameters r_f and r_u. Provided that the acceptor can be selectively excited in the presence of the donor, the normalized fluorescence quantum yield of the acceptor as a function of the denaturant (e.g., urea) can be determined:

$$\frac{F_{Denaturant}}{F_0} = \left[\frac{Q_{A,f} + K_{eq} Q_{A,u}}{1 + K_{eq}} \right]_{Denaturant} \Big/ \left[\frac{Q_{A,f} + K_{eq} Q_{A,u}}{1 + K_{eq}} \right]_0 \qquad (6)$$

where F_0 is the integrated fluorescence intensity of the acceptor in the absence of denaturant. The quantum yield of the acceptor and the folding free energy

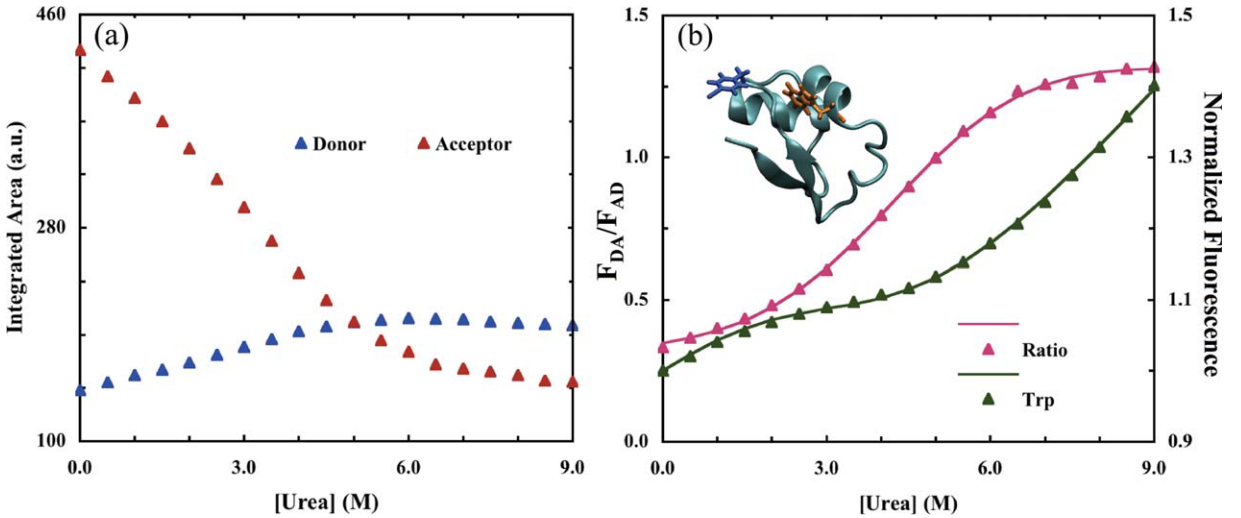

Figure 2. (a) Phe_{CN}-Trp FRET data obtained with the LysM domain (pdb code: 1E0G) and (b) the corresponding F_{DA} to F_{AD} ratios at different urea concentrations. The locations of the Phe_{CN} (blue) and Trp (orange) are shown in the inset of (b). Also shown in (b) is the normalized fluorescence intensity of Trp, measured on direct excitation at 290 nm. Smooth lines are global fits to these data according to the methods discussed in the text, yielding the following parameters: $r_f = 13.0$ Å, $r_u = 16.4$ Å, and $\Delta G^0(0) = 1.4$ kcal/mol. The latter is comparable to that (1.2 kcal/mol) determined via CD spectroscopy.[77] (Adapted from Glasscock JM, et al., (2008) Biochemistry 47:11070–12076, with permission from American Chemical Society.)

are furthermore assumed to be linear functions of denaturant concentration:

$$Q_{A,u} = Q^0_{A,u} + q.[x] \quad (7)$$

$$\Delta G^0(x) = \Delta G^0(0) + m.[x] \quad (8)$$

The six fitting parameters (i.e., $\Delta G^\circ(0)$, m, $Q^0_{A,u}$, r_f, r_u, and q) in Eqs. (5–8) are used to globally fit the measured curves of F_{DA}/F_{AD} and $F_{Denaturant}/F_0$ as a function of urea concentration x. As shown (Fig. 2), using this approach Glasscock *et al.*[77] showed that the free energy of unfolding as well as the donor-to-acceptor separation distance in the folded state of the LysM domain were in good agreement with those found by alternative spectroscopic methods,[77,78] even under the simplifying assumption that $P(r)$ is a delta function in the unfolded state.

Another interesting application of FRET is its use in extracting chain dynamics of biopolymers. For such studies, however, it is most useful to choose a donor with a long fluorescence lifetime, as backbone motions that move the FRET pair closer or farther apart modulate the energy transfer rate, k_T, according to:

$$k_T = \frac{1}{\tau_D}\left(\frac{R_0}{r}\right)^6 \quad (9)$$

where τ_D is the donor fluorescence lifetime in the absence of acceptor. Thus, long-range intrachain diffusive motions lead to complex, nonsingle-exponential decay of the donor fluorescence. The time dependent probability of finding a donor in its excited state at a distance r from the acceptor can be described by the following equation[79,80]:

$$\frac{\partial \overline{P}(r,t)}{\partial t} = -\frac{1}{\tau_D}\left\{\left(1+\left(\frac{R_0}{r}\right)^6\right)\overline{P}(r,t)\right\} + \frac{1}{P(r)}\frac{\partial}{\partial(r)}\left(P(r)D_{DA}\frac{\partial \overline{P}(r,t)}{\partial r}\right) \quad (10)$$

with $\overline{P}(r,t) = P(r,t)/P(r)$. The first term in Eq. (10) represents the distance dependence of the FRET signal, whereas the second term accounts for intrachain diffusive motions with a diffusion coefficient D_{AD}. To probe both the equilibrium distance distribution, $P(r)$, and D_{AD} for flexible biopolymers, one can measure the donor fluorescence decay while varying one or more properties such as τ_D or the solvent viscosity. For example, by using the naphthalene/dansyl and pyrene/dansyl FRET pairs, Kiefhaber and coworkers[81] used the latter approach to probe the end-to-end distance distribution and chain dynamics of poly(Gly–Ser) chains. The fluorescence lifetimes of naphthalene (~36.9 ns) and pyrene (~225.5 ns) dyes in water are significantly different, but their Förster radii are very similar, with 23.3 and 20.5 Å for the naphthalene/dansyl and pyrene/dansyl FRET pairs, respectively. Thus, by fitting the experimental data to Eq. (10) and using a model for $P(r)$, information about both the distance distribution and D_{AD} were determined.

Although FRET pairs based on fluorescent dyes have been extensively used in biological and biophysical studies, applying them to studies involving natively folded proteins could be problematic as they tend to be large, thus greatly destabilizing and possibly altering their folded states. Thus, we and others have developed a range of FRET pairs that are amino acid-like in nature, and thus minimally perturb the

Table I. *Unnatural Amino Acid-Based FRET Pairs*

Donor	Acceptor	R_0 (Å)	Ref.
p-Cyanophenylalanine	Tryptophan	16.0	68
p-Cyanophenylalanine	Tyrosine	12.0	71
p-Cyanophenylalanine	5-Hydroxytryptophan	18.5	84
p-Cyanophenylalanine	5-Cyanotryptophan	n.d.	82
p-Ethynylphenylalanine	Tryptophan	n.d.	83
p-Cyanophenylalanine	7-Azatryptophan	18.5	84
p-Cyanophenylalanine	Thioamide	15.6	85

energetic and structural properties of the protein and peptide systems in question.[68,71,82–85] As shown (Table I), these FRET pairs are mostly analogs of amino acid sidechains, making them ideally suited for probing conformational distributions and transitions of peptides and small proteins, as well as conformational changes occurring over a relatively short distance. Moreover, and perhaps more importantly, these FRET pairs could be used as a starting point for constructing multi-FRET systems, allowing more structural information to be extracted from a single FRET experiment. For example, Rogers *et al.*[84] have shown that Phe_{CN}, Trp, and 7-azatryptophan (7AW) can be used together to form a two-step FRET system and have utilized it to investigate the denaturant induced unfolding of the WW domain.

Triplet state and fluorescence quenching

Similar to FRET, other types of quenching mechanisms that lead to shortening of either the excited singlet or triplet state lifetimes have also found very important applications in protein folding studies. Unlike FRET, however, such quenching processes occur only over a very short distance, that is, typically only on formation of van der Waals contacts between the chromophore and quencher.[86,87] For example, for a simple loop closure process (i.e., open (*O*) to closed (*C*) state), the kinetics of quenching can be described by the following scheme:

$$O \underset{k_{cl}}{\overset{k_{op}}{\rightleftarrows}} C \xrightarrow{k_{TT}} {}^{D}C$$

where k_{TT} is the quenching rate in the closed state, whereas k_{op} and k_{cl} are the intrinsic opening and closing rates of the loop. It can be shown that if the rate of quenching is much larger than the rate of opening (i.e., $k_{TT} \gg k_{op}$) then the observed rate constant corresponds to the rate of closing. Several research groups have utilized such quenching methods,[88–90] especially quenchers of the triplet state of Trp (Table II), to investigate peptide loop closure rates,[89–91] native state conformational fluctuations,[92] and global cooperative folding/unfolding transitions.[93]

Recently, fluorescence correlation spectroscopy (FCS) has become increasingly used as a tool to investigate the dynamics of protein folding and conformational changes.[94–102] FCS is based on correlating the fluorescence intensity fluctuations of the molecular species in question induced by either a fluorescence quenching event or by molecular diffusion in and out of a small confocal laser excitation volume. For example, Sauer and coworkers[103,104] have shown that the fluorescence of oxazine dyes can be effectively quenched by Trp through the mechanism of photoinduced electron transfer (PET), making them ideal for use as probes of peptide and protein dynamics by means of FCS[105,106] More recently, Rogers *et al.*[107] have applied the PET-FCS technique, wherein the fluorescence of the dye Atto 655 is effectively quenched by nearby Trp residues, to reveal the conformational dynamics of a truncated version (M2TM) of the Influenza A M2 proton channel in model membranes and found that the conformational transition between the N-terminally open and C-terminally open states of the M2TM channel occurs on a timescale of about 500 μs.

Linear IR spectroscopy

Vibrational transitions in condensed phase occur on fs and/or ps timescales, thus IR spectroscopy can be used to investigate ultrafast conformational events of biological molecules. For proteins and peptides, IR bands arising from backbone vibrations are particularly useful as they show varying degrees of sensitivity to conformations.[108] Due to having the largest intensity, however, the amide I band, which originates mostly from the stretching vibrations of backbone carbonyls, is the most widely used as a probe of protein folding.[109–116] The conformational sensitivity of the backbone amide vibrational transitions arises from anharmonic interactions between the different vibrators located on different amide groups.[117,118] The underlying theoretical framework is often represented in terms of an *N*-dimensional Hamiltonian written in the basis of the N number of free floating vibrators located at the positions of the corresponding backbone amide groups:

$$H = \begin{pmatrix} \varepsilon_1 & \Delta_{12} & \Delta_{13} & \cdots \\ \Delta_{21} & \varepsilon_2 & \Delta_{23} & \cdots \\ \Delta_{31} & \Delta_{32} & \cdots & \Delta_{N-1,N} \\ \cdots & \cdots & \Delta_{N,N-1} & \varepsilon_N \end{pmatrix} \quad (11)$$

where ε_i is the unperturbed frequency of the *i*th oscillator, and Δ_{ij} is the interaction energy between

Table II. *Tryptophan Triplet State Quenchers*

Quencher	Quenching rate constant (M^{-1} S^{-1})	Ref.
3-Nitro-tyrosine	7×10^9	88
Tryptophan	2.1×10^8	89
Cysteine	1.3×10^8	89
Cystine	1.9×10^8	89
Lipoate	$1.4 \times \cdot 0^9$	89
Naphtylalanine	3×10^9	90

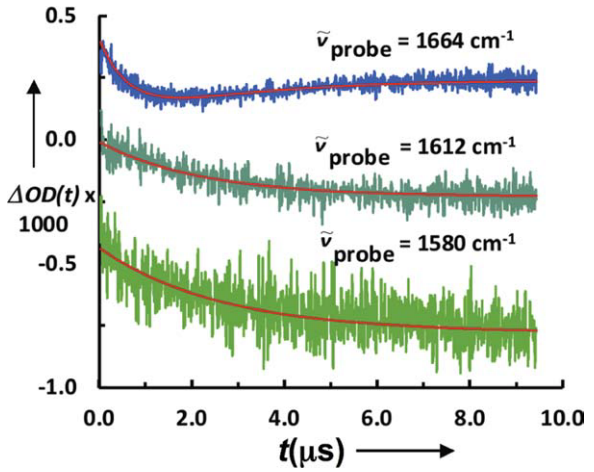

Figure 3. Conformational relaxation kinetics of a Trp-cage in response to a *T*-jump obtained with different probing frequencies, showing that folding intermediates or kinetic heterogeneity could be revealed by recording transient IR kinetics over the entire amide I′ band region. (Adapted from Culik RM, et al., (2011) Angew Chem Int Ed 50:10884–10887, with permission from John Wiley and Sons.)[127]

the *i*th and *j*th vibrators. Although experimentally determining Δ_{ij} is not straightforward, it is generally assumed that long range electrostatic interactions play a dominant role, while through-bond contributions may be important for nearest neighbor terms.[119,120] Because both ε_i and Δ_{ij} are sensitive to various environmental and structural factors, the resulting IR band shows a dependence on the protein conformation and hydration status.[121,122] For example, in D_2O the amide I′ band of solvated α-helices is centered at ~1630 cm^{-1},[11] whereas that of antiparallel β-sheets consists of two bands at ~1620 cm^{-1} (strong) and ~1680 cm^{-1} (weak),[117] respectively.

In conjunction with laser-induced *T*-jump techniques, time-resolved IR measurements have significantly enhanced our understanding of the folding dynamics of protein secondary structures in isolation[123,124] and in various mini-proteins.[125–127] For example, Dyer and coworkers[7] are among the first to show that, following a *T*-jump, the conformation relaxation of short alanine-based α-helical peptides, probed by IR spectroscopy, occurs on the ns timescale. In addition, application of the *T*-jump IR technique to the study of β-hairpin folding dynamics has allowed us to substantiate the idea that turn formation is the rate limiting step in β-hairpin folding[128–130] and helix–turn–helix formation.[131,132] More recently, we have shown, using the miniprotein Trp-cage[133,134] as an example (Fig. 3), that *T*-jump IR measurements carried out using different probing frequencies within the amide I′ band of the protein of interest can reveal important information regarding the individual folding rates of the constituent structural elements.[127]

Strategies to enhance the structural resolution of IR spectroscopy

Although the aforementioned couplings among different amide vibrators provide the intrinsic sensitivity of the amide I vibration to protein conformation, it also causes the transition to broaden. In addition, the amide I frequencies of different secondary structures are not well separated. As a result, the amide I band of proteins is often broad, featureless, and congested with overlapping peaks. Thus, to gain site-specific structural information, certain strategies need to be used. One such strategy is to alter the reduced mass and hence the vibrational frequency of the vibrator of interest using isotopic substitution.[135–138] For example, assuming that the backbone C=O stretching vibration is harmonic, simply changing ^{12}C to ^{13}C would lead to a decrease in its vibration frequency by approximately 40 cm^{-1}, making it possible to separate the ^{13}C=O vibration from a background arising from unlabeled (i.e., ^{12}C=O) vibrators (Fig. 4). Therefore, the technique of isotope editing has been widely used in protein folding and aggregation studies to gain a better structural resolution when used in conjunction with IR spectroscopy.[113,139]

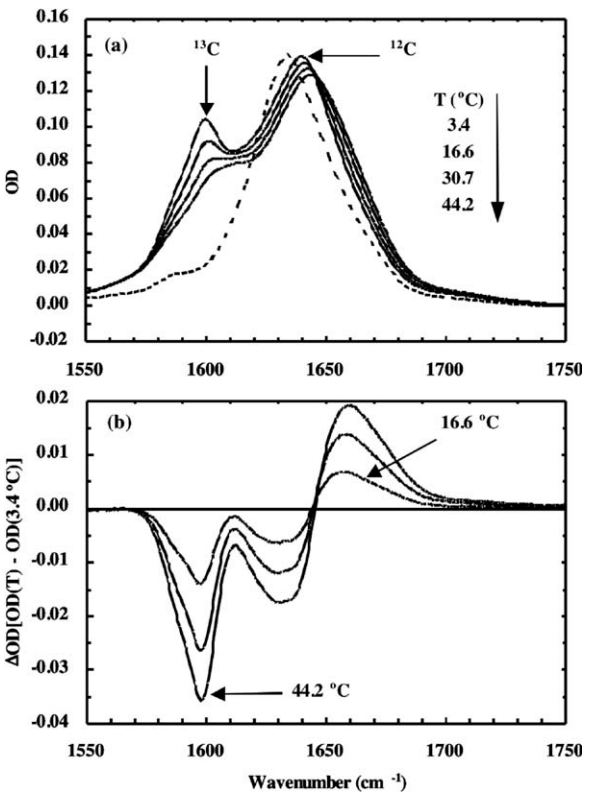

Figure 4. (a) FTIR spectra of a ^{13}C labeled (solid lines) in D_2O solution measured at different temperatures and (b) the corresponding difference FTIR spectra. Also shown in (a) is the FTIR spectrum (dashed line) of the unlabeled peptide. (Reprinted from Huang CY, et al., (2001) J Am Chem Soc 123:12111–12112, with permission from American Chemical Society.)[139]

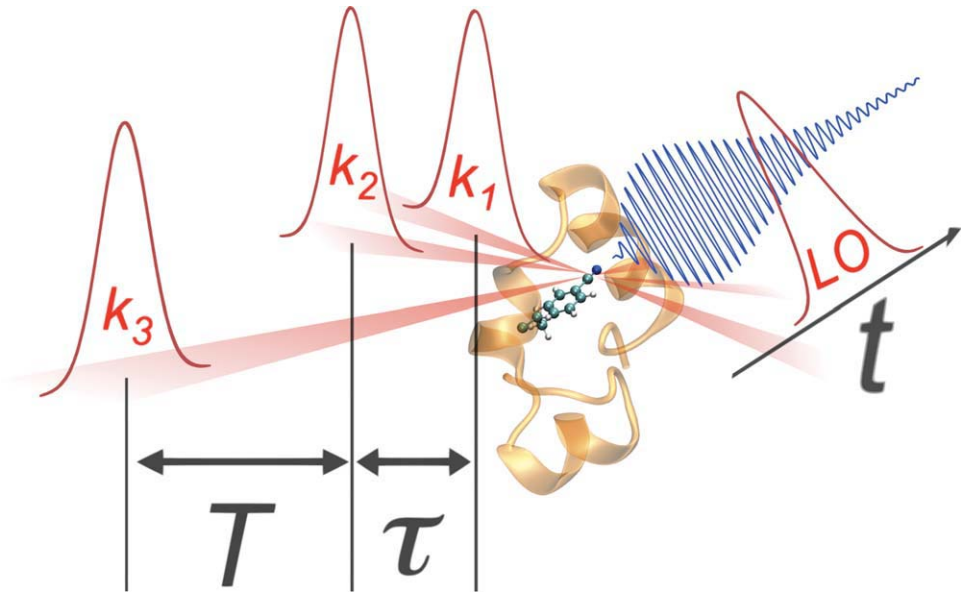

Figure 5. Schematic representation of the 2D IR photon echo experiment. Three ultrashort IR pulses (k_1, k_2 and k_3) interact in succession with a protein sample to produce a photon echo signal (depicted in blue), which is analyzed along the time axis t by overlapping with a reference pulse (LO).

In addition to backbone vibrations, many sidechain vibrations are also expected to be useful IR markers of protein conformations. However, sidechain vibrations are much less used in protein folding studies due in part to their smaller molar extinction coefficients. Exceptions include the carboxylate asymmetric stretching vibrations of the Glu and Asp sidechains, which possess strong absorptions appearing near 1567 and 1584 cm^{-1}, respectively.[114] On protonation of these sidechains at low pH, the corresponding vibrations shift to near 1700 cm^{-1}. Thus, these sidechain absorptions could be used as sensitive IR probes of local pH as well as salt bridge and ion pair formations. Moreover, we and others have recently demonstrated a novel method to enhance the structural resolution in IR studies by using unnatural amino acids as site-specific environmental and conformational reporters. Interested readers can find more details of this topic in a recent review.[140]

UV resonance Raman

Protein vibrational transitions can also be probed via Raman spectroscopy. It has been shown that excitation of an electronic transition of the polypeptide using deep UV photons, for example the $\pi \rightarrow \pi^*$ transition of the amide backbone or the ^1L_b transition of Trp residues, allows resonantly enhanced Raman spectra to be collected.[141–145] In comparison to IR measurements, which often suffer from interference of solvent vibrational bands in the amide II and III regions, the UV resonance Raman (UVRR) technique can greatly reduce solvent interferences, thus allowing for more easy recording of protein vibrational bands below 1600 cm^{-1}, for example, the amide III band and the C_α—H stretching vibration. The ability to reliably record protein vibrational spectrum in the lower wavenumber region makes UVRR a very useful tool of reporting on protein conformations. For example, Asher *et al.*[146] have proposed that the amide III peak frequency shows a roughly sinusoidal dependence on the backbone Psi angle, making a more quantitative interpretation of the vibrational spectrum possible. In addition, UVRR has also been used in conjunction with the laser-induced *T*-jump technique to study protein and peptide folding kinetics.[147–151] Further details on the application of UVRR to protein folding studies can be found in a recent review by Asher and coworkers.[145]

Nonlinear IR methods

Probing the nonlinear response of a protein sample induced by a series of ultrashort laser pulses can provide additional dynamic and structural information that cannot be directly acquired via linear spectroscopic measurements. In particular, 2-dimensional infrared (2D-IR) spectroscopy has proven to be very useful in generating new insights into the ultrafast conformational and solvation dynamics of proteins and peptides[152–154] and is expected to play a growing role in studying the protein folding problem.

Because a detailed description of the 2D-IR technique can be found elsewhere,[155] below we offer only a brief description. As shown (Fig. 5), one common method for generating 2D-IR spectra makes use of four ultrashort (<100 fs), phase locked, IR laser pulses that may have different polarizations and are delayed in time with respect to each other. The first pulse (k_1) is used to promote the sample vibration into a superposition of the ground and excited states (or to produce a coherence), which is intersected by

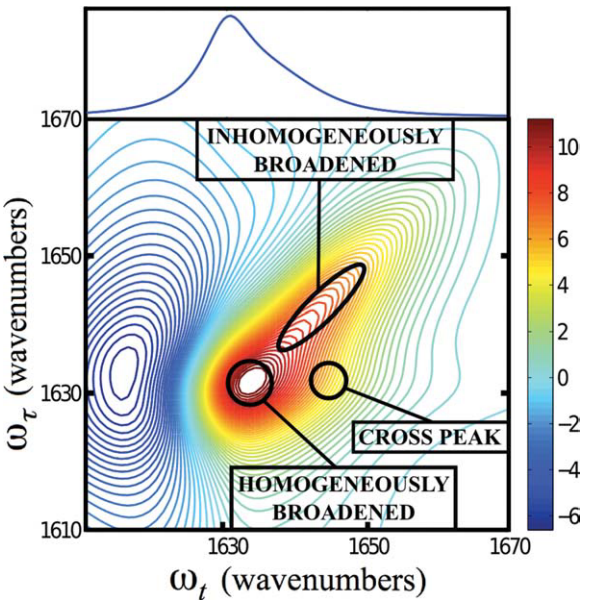

Figure 6. A representation of the 2D-IR photon echo spectrum (bottom) for two interacting anharmonic vibrators, demonstrating characteristic features that distinguish it from the linear IR spectrum (top) such as the appearance of well-defined homogeneously or inhomogeneously broadened peaks, as well as cross peaks arising from coupling.

a second pulse (k_2) at a certain time delay, τ, generating a transient population grating that is then allowed to interact with a third pulse (k_3) after a delay time T, stimulating emission of a photon echo signal.[156] The magnitude and phase of the photon echo are then determined through interference with a fourth pulse, the local oscillator (LO), along the detection time axis, t. Finally, Fourier analysis of this signal along the two time axes, τ and t, produces the 2D-IR spectrum, which is a function of two frequencies, ω_τ and ω_t, and the mixing time T. One of the advantages of 2D-IR spectroscopy is that it allows one to spread the spectrum of interest into two dimensions, thus effectively increasing the spectral resolution by revealing features that overlap, cancel, or simply do not exist in linear IR spectra.[157] As shown (Fig. 6), a 2D-IR spectrum can also reveal cross correlations between frequencies that go undetected in linear IR spectroscopy, thus providing additional structural information.[156] Moreover, by following the evolution of the spectral line-widths in 2D spectra as a function of T, one can measure ultrafast (ps) dynamics due to solvent or peptide motions.[158] Additionally, 2D-IR signals show a fourth-power dependence on the underlying vibrational transition dipole moment (i.e., proportional to μ^4), allowing for enhanced discrimination of overlapping IR bands.[159]

Taken together, these added spectral and dynamic details contained in the nonlinear response of a protein makes 2D-IR spectroscopy a more sensitive structural tool for studying protein folding, conformational transitions, and local hydration status, among many other applications. For example, Hochstrasser and coworkers[160] have used the 2D-IR technique to study the conformational heterogeneity of HP35 via the C≡N (nitrile) stretching vibration of Phe_{CN} incorporated into the hydrophobic core of the protein. It was found that the 2D-IR spectra could only be described by two nearly overlapping distributions of vibrators that do not interconvert on a timescale similar to the range of T (0–3 ps). Because the nitrile stretching vibration is sensitive to hydration, this finding provided strong evidence that in the native potential well of HP35 two or more slowly interconverting subpopulations exist. A similar conclusion was also arrived at by a triplet–triplet state quenching study.[92]

Although much progress is left to be made in the implementation of nonlinear spectroscopic methods such as 2D-IR spectroscopy to protein folding studies, several previous works stand out so far as showing their potential usefulness. For example, a large amount of effort has been made to characterize the 2D-IR spectral features of different secondary structural motifs,[161–165] laying the foundation for interpreting 2D-IR data of more complex protein systems. In addition, a small number of protein folding kinetic studies[46,166–168] have demonstrated that when combined with other resolution enhancement strategies, such as isotope-editing, 2D-IR spectroscopy is capable of revealing details regarding the folding/unfolding dynamics of the protein system of interest that are inaccessible from linear spectroscopy methods. With the development of other light-induced triggering methods,[64] and continuing refinement of the experimental methods,[169] we expect that multidimensional nonlinear spectroscopies will serve as critical tools in providing new mechanistic insights into protein folding dynamics.

Summary

The problem of protein folding has inspired a vast variety of studies by scientists from different disciplines in the past and continues to stimulate the development of new experimental methods that can measure and report, with as much structural detail as possible, on how and on what range of timescales specific and/or nonspecific conformational transitions occur. In particular, the development and application of various ultrafast triggering methods, such as the laser-induced T-jump technique, have made it possible to directly characterize the folding kinetics and mechanism of protein secondary structures and proteins that fold on the nanosecond and microsecond timescales. In addition, and perhaps more importantly, the recent advances in vibrational and optical spectroscopies hold great promise for disentangling and even "imaging" the complex network of molecular interactions involved in protein folding. Herein,

we provide a concise summary of several recent developments in spectroscopic studies of protein folding, with the hope that it will provide useful information to those interested in applying some of the aforementioned methods to protein conformational studies. Due to page limit, however, we are unable to discuss several other deserving spectroscopic methods, such as those based on single-molecule fluorescence and/or FRET measurements. Finally, it is worth noting that many of those spectroscopic methods discussed are not limited to protein folding studies, they can also be applied to investigate other biophysical and biological questions, such as aggregation,[170–173] membrane protein conformation and dynamics,[174–178] peptide–peptide interactions, RNA and DNA dynamics,[179–182] and structure determination.[154]

References

1. Anfinsen CB (1973) Principles that govern folding of protein chains. Science 181:223–230.
2. Chan CK, Hu Y, Takahashi S, Rousseau DL, Eaton WA, Hofrichter J (1997) Submillisecond protein folding kinetics studied by ultrarapid mixing. Proc Natl Acad Sci USA 94:1779–1784.
3. Roder H, Maki K, Cheng H (2006) Early events in protein folding explored by rapid mixing methods. Chem Rev 106:1836–1861.
4. Nitzan A (2006) Chemical dynamics in condensed phases: relaxation, transfer, and reactions in condensed molecular systems. New York: Oxford University Press Inc.
5. Beitz JV, Flynn GW, Turner DH, Sutin N (1970) Stimulated Raman effect—a new source of laser temperature-jump heating. J Am Chem Soc 92:4130–7296.
6. Phillips CM, Mizutani Y, Hochstrasser RM (1995) Ultrafast thermally-induced unfolding of RNase-A. Proc Natl Acad Sci USA 92:7292–7296.
7. Williams S, Causgrove TP, Gilmanshin R, Fang KS, Callender RH, Woodruff WH, Dyer RB (1996) Fast events in protein folding: helix melting and formation in a small peptide. Biochemistry 35:691–697.
8. Ballew RM, Sabelko J, Gruebele M (1996) Direct observation of fast protein folding: the initial collapse of apomyoglobin. Proc Natl Acad Sci USA 93:5759–5764.
9. Thompson PA, Eaton WA, Hofrichter J (1997) Laser temperature jump study of the helix reversible arrow coil kinetics of an alanine peptide interpreted with a 'kinetic zipper' model. Biochemistry 36:9200–9210.
10. Gruebele M, Sabelko J, Ballew R, Ervin J (1998) Laser temperature jump induced protein refolding. Acc Chem Res 31:699–707.
11. Dyer RB, Gai F, Woodruff WH (1998) Infrared studies of fast events in protein folding. Acc Chem Res 31: 709–716.
12. Mohammed OF, Jas GS, Lin MM, Zewail AH (2009) Primary peptide folding dynamics observed with ultrafast temperature jump. Angew Chem Int Ed 48: 562856–562832.
13. Metzler R, Klafter J, Jortner J, Volk M (1998) Multiple time scales for dispersive kinetics in early events of peptide folding. Chem Phys Lett 293:477–484.
14. Wang J, El-Sayed MA (1999) Temperature jump-induced secondary structural change of the membrane protein bacteriorhodopsin in the premelting temperature region: a nanosecond time-resolved Fourier transform infrared study. Biophys J 76:2777–2783.
15. Ansari A, Kuznetsov SV, Shen Y (2001) Configurational diffusion down a folding funnel describes the dynamics of DNA hairpins. Proc Natl Acad Sci USA 98:7771–7776.
16. Qiu L, Pabit SA, Roitberg AE, Hagen SJ (2002) Smaller and faster: the 20-residue trp-cage protein folds in 4 μs. J Am Chem Soc 124:12952–12953.
17. Mayor U, Guydosh NR, Johnson CM, Grossmann JG, Sato S, Jas GS, Freund SMV, Alonso DOV, Daggett V, Fersht AR (2003) The complete folding pathway of a protein from nanoseconds to microseconds. Nature 421:863–867.
18. Ferguson N, Fersht AR (2003) Early events in protein folding. Curr Opin Struct Biol 13:75–81.
19. Sadqi M, Lapidus LJ, Munoz V (2003) How fast is protein hydrophobic collapse?Proc Natl Acad Sci USA 100:12117–12122.
20. Munoz V, Ghirlando R, Blanco FJ, Jas GS, Hofrichter J, Eaton WA (2006) Folding and aggregation kinetics of a β-hairpin. Biochemistry 45:7023–7035.
21. Callender R, Dyer RB (2006) Advances in time-resolved approaches to characterize the dynamical nature of enzymatic catalysis. Chem Rev 106:3031–3042.
22. Khuc MT, Mendonca L, Sharma S, Solinas X, Volk M, Hache F (2011) Measurement of circular dichroism dynamics in a nanosecond temperature-jump experiment. Rev Sci Instrum 82:054302.
23. Buchner GS, Murphy RD, Buchete N, Kubelka J (2011) Dynamics of protein folding: probing the kinetic network of folding–unfolding transitions with experiment and theory. Biochim Biophys Acta 1814: 1001–1020.
24. Lednev IK, Ye TQ, Hester RE, Moore JN (1996) Femtosecond time-resolved UV-visible absorption spectroscopy of trans-azobenzene in solution. J Phys Chem 100:13338–13341.
25. Nagele T, Hoche R, Zinth W, Wachtveitl J (1997) Femtosecond photoisomerization of cis-azobenzene. Chem Phys Lett 272:489–495.
26. Kumita JR, Smart OS, Woolley GA (2000) Photo-control of helix content in a short peptide. Proc Natl Acad Sci USA 97:3803–3808.
27. Flint DG, Kumita JR, Smart OS, Woolley GA (2002) Using an azobenzene cross-linker to either increase or decrease peptide helix content upon trans-to-cis photoisomerization. Chem Biol 9:391–397.
28. Renner C, Kusebauch U, Loweneck M, Milbradt AG, Moroder L (2005) Azobenzene as photoresponsive conformational switch in cyclic peptides. J Peptide Res 65:4–14.
29. Wachtveitl J, Sporlein S, Satzger H, Fonrobert B, Renner C, Behrendt R, Oesterhelt D, Moroder L, Zinth W (2004) Ultrafast conformational dynamics in cyclic azobenzene peptides of increased flexibility. Biophys J 86:2350–2362.
30. Beharry AA, Woolley GA (2011) Azobenzene photoswitches for biomolecules. Chem Soc Rev 40:4422–4437.
31. Hamm P, Helbing J, Bredenbeck J (2008) Two-dimensional infrared spectroscopy of photoswitchable peptides. Annu Rev Phys Chem 59:291–317.
32. Backus EHG, Bloem R, Donaldson PM, Ihalainen JA, Pfister R, Paoli B, Caflisch A, Hamm P (2010) 2D-IR study of a photoswitchable isotope-labeled α-helix. J Phys Chem B 114:3735–3740.
33. Sporlein S, Carstens H, Satzger H, Renner C, Behrendt R, Moroder L, Tavan P, Zinth W, Wachtveitl J

(2002) Ultrafast spectroscopy reveals subnanosecond peptide conformational dynamics and validates molecular dynamics simulation. Proc Natl Acad Sci USA 99:7998–8002.
34. Bredenbeck J, Helbing J, Kumita JR, Woolley GA, Hamm P (2005) α-Helix formation in a photoswitchable peptide tracked from picoseconds to microseconds by time-resolved IR spectroscopy. Proc Natl Acad Sci USA 102:2379–2384.
35. Ihalainen JA, Paoli B, Muff S, Backus EHG, Bredenbeck J, Woolley GA, Caflisch A, Hamm P (2008) α-Helix folding in the presence of structural constraints. Proc Natl Acad Sci USA 105:9588–9593.
36. Xie S, Natansohn A, Rochon P (1993) Recent developments in aromatic azo polymers research. Chem Mater 5:403–411.
37. Tamai N, Miyasaka H (2000) Ultrafast dynamics of photochromic systems. Chem Rev 100:1875–1890.
38. Natansohn A, Rochon P (2002) Photoinduced motions in azo-containing polymers. Chem Rev 102:4139–4175.
39. Pelliccioli AP, Wirz J (2002) Photoremovable protecting groups: reaction mechanisms and applications. Photochem Photobiol Sci 1:441–458.
40. Haines LA, Rajagopal K, Ozbas B, Salick DA, Pochan DJ, Schneider JP (2005) Light-activated hydrogel formation via the triggered folding and self-assembly of a designed peptide. J Am Chem Soc 127:17025–17029.
41. Hirota S, Fujimoto Y, Choi J, Baden N, Katagiri N, Akiyama M, Hulsker R, Ubbink M, Okajima T, Takabe T, Funasaki N, Watanabe Y, Terazima M (2006) Conformational changes during apoplastocyanin folding observed by photocleavable modification and transient grating. J Am Chem Soc 128:7551–7558.
42. Sankaranarayanan J, Muthukrishnan S, Gudmundsdottir AD (2009) Photoremovable protecting groups based on photoenolization. Adv Phys Org Chem 43 43:39–77.
43. Chen H, Hsu JC, Man Hoang Viet, Li MS, Hu C, Liu C, Luh FY, Chen SS, Chang ES, Wang AH, Hsu M, Fann W, Chen RP (2010) Studying submicrosecond protein folding kinetics using a photolabile caging strategy and time-resolved photoacoustic calorimetry. Proteins 78:2973–2983.
44. Hansen KC, Rock RS, Larsen RW, Chan SI (2000) A method for photoinitating protein folding in a nondenaturing environment. J Am Chem Soc 122:11567–11568.
45. Lu HSM, Volk M, Kholodenko Y, Gooding E, Hochstrasser RM, DeGrado WF (1997) Aminothiotyrosine disulfide, an optical trigger for initiation of protein folding. J Am Chem Soc 119:7173–180.
46. Kolano C, Helbing J, Kozinski M, Sander W, Hamm P (2006) Watching hydrogen-bond dynamics in a β-turn by transient two-dimensional infrared spectroscopy. Nature 444:469–472.
47. Kolano C, Helbing J, Bucher G, Sander W, Hamm P (2007) Intramolecular disulfide bridges as a phototrigger to monitor the dynamics of small cyclic peptides. J Phys Chem B 111:11297–11302.
48. Waegele MM (2011) On the folding and conformation of peptides and the development of novel methods for their study. Publicly accessible Penn Dissertations.
49. Prompers JJ, Hilbers CW, Pepermans HAM (1999) Tryptophan mediated photoreduction of disulfide bond causes unusual fluorescence behavior of Fusarium solani pisi cutinase. FEBS Lett 456:409–416.
50. Neves-Petersen MT, Gryczynski Z, Lakowicz J, Fojan P, Pedersen S, Petersen E, Petersen SB (2002) High probability of disrupting a disulphide bridge mediated by an endogenous excited tryptophan residue. Protein Sci 11:588–600.
51. Vanhooren A, Devreese B, Vanhee K, Van Beeumen J, Hanssens I (2002) Photoexcitation of tryptophan groups induces reduction of two disulfide bonds in goat α-lactalbumin. Biochemistry 41:11035–11043.
52. Kehoe JJ, Remondetto GE, Subirade M, Morris ER, Brodkorb A (2008) Tryptophan-mediated denaturation of β-lactoglobulin A by UV irradiation. J Agric Food Chem 56:4720–4725.
53. Wu LZ, Sheng YB, Xie JB, Wang W (2008) Photoexcitation of tryptophan groups induced reduction of disulfide bonds in hen egg white lysozyme. J Mol Struct 882:101–106.
54. Neves-Petersen MT, Klitgaard S, Pascher T, Skovsen E, Polivka T, Yartsev A, Sundstrom V, Petersen SB (2009) Flash photolysis of cutinase: identification and decay kinetics of transient intermediates formed upon UV excitation of aromatic. Biophys J 97:211–226.
55. Mines GA, Pascher T, Lee SC, Winkler JR, Gray HB (1996) Cytochrome c folding triggered by electron transfer. Chem Biol 3:491–497.
56. Gray HB, Winkler JR (1996) Electron transfer in proteins. Annu Rev Biochem 65:537–561.
57. Ansari A, Berendzen J, Bowne SF, Frauenfelder H, Iben IE, Sauke TB, Shyamsunder E, Young RD (1985) Protein states and protein quakes. Proc Natl Acad Sci USA 82:5000–5004.
58. Jones CM, Henry ER, Hu Y, Chan CK, Luck SD, Bhuyan A, Roder H, Hofrichter J, Eaton WA (1993) Fast events in protein-folding initiated by nanosecond laser photolysis. Proc Natl Acad Sci USA 90:11860–11864.
59. Chen E, Goldbeck RA, Kliger DS (1997) Nanosecond time-resolved spectroscopy of biomolecular processes. Annu Rev Biophys Biomol Struct 26:327–355.
60. Eaton WA, Munoz V, Hagen JS, Jas GS, Lapidus LJ, Henry ER, Hofrichter J (2000) Fast kinetics and mechanisms in protein folding. Annu Rev Biophys Biomol Struct 29:327–359.
61. Tucker MJ, Courter JR, Chen J, Atasoylu O, Smith, Amos B., III, Hochstrasser RM (2010) Tetrazine phototriggers: probes for peptide dynamics. Angew Chem Int Ed 49:3612–3616.
62. Mukamel S (1995) Principles of nonlinear optical spectroscopy, Oxford Press, New York.
63. Chen Y, Barkley MD (1998) Toward understanding tryptophan fluorescence in proteins. Biochemistry 37: 9976–9982.
64. Gruebele M (1999) The fast protein folding problem. Annu Rev Phys Chem 50:485–516.
65. Engelborghs Y (2001) The analysis of time resolved protein fluorescence in multi-tryptophan proteins. Spectrochim Acta Part A 57:2255–2270.
66. Royer CA (2006) Probing protein folding and conformational transitions with fluorescence. Chem Rev 106:1769–1784.
67. Zhong D (2009) Hydration dynamics and coupled water–protein fluctuations probed by intrinsic tryptophan. Adv Chem Phys 143:83–149.
68. Tucker MJ, Oyola R, Gai F (2006) A novel fluorescent probe for protein binding and folding studies: p-cyanophenylalanine. Biopolymers 83:571–576.
69. Serrano AL, Troxler T, Tucker MJ, Gai F (2010) Photophysics of a fluorescent non-natural amino acid: p-cyanophenylalanine. Chem Phys Lett 487:303–306.
70. Marek P, Mukherjee S, Zanni MT, Raleigh DP (2010) Residue-specific, real-time characterization of lag-phase species and fibril growth during amyloid formation: a combined fluorescence and IR study of p-cyanophenylalanine analogs of islet amyloid polypeptide. J Mol Biol 400:878–888.

71. Taskent-Sezgin H, Marek P, Thomas R, Goldberg D, Chung J, Carrico I, Raleigh DP (2010) Modulation of p-cyanophenylalanine fluorescence by amino acid side chains and rational design of fluorescence probes of α-helix formation. Biochemistry 49:6290–6295.
72. Tang J, Yin H, Qiu J, Tucker MJ, DeGrado WF, Gai F (2009) Using two fluorescent probes to dissect the binding, insertion, and dimerization kinetics of a model membrane peptide. J Am Chem Soc 131: 3816–3817.
73. Noomnarm U, Clegg RM (2009) Fluorescence lifetimes: fundamentals and interpretations. Photosynthesis Res 101:181–194.
74. Haas E (2005) The study of protein folding and dynamics by determination of intramolecular distance distributions and their fluctuations using ensemble and single-molecule FRET measurements. Chemphyschem 6:858–970.
75. Lakowicz JR (1999) Principles of fluorescence spectroscopy. New York: Springer.
76. Berney C, Danuser G (2003) FRET or no FRET: a quantitative comparison. Biophys J 84:3992–4010.
77. Glasscock JM, Zhu Y, Chowdhury P, Tang J, Gai F (2008) Using an amino acid fluorescence resonance energy transfer pair to probe protein unfolding: application to the villin headpiece subdomain and the LysM domain. Biochemistry 47:11070–12076.
78. Nickson AA, Stoll KE, Clarke J (2008) Folding of a LysM domain: entropy–enthalpy compensation in the transition state of an ideal two-state folder. J Mol Biol 380:557–569.
79. Haas E, Katchalski-Katzir E, Steinberg I (1978) Brownian-motion of ends of oligopeptide chains in solution as estimated by energy-transfer between chain ends. Biopolymers 17:11–31.
80. Beechem JM, Haas E (1989) Simultaneous determination of intramolecular distance distributions and conformational dynamics by global analysis of energy-transfer measurements. Biophys J 55:1225–1236.
81. Moglich A, Joder K, Kiefhaber T (2006) End-to-end distance distributions and intrachain diffusion constants in unfolded polypeptide chains indicate intramolecular hydrogen bond formation. Proc Natl Acad Sci USA 103:12394–12399.
82. Waegele MM, Tucker MJ, Gai F (2009) 5-Cyanotryptophan as an infrared probe of local hydration status of proteins. Chem Phys Lett 478:249–253.
83. Miyake-Stoner SJ, Miller AM, Hammill JT, Peeler JC, Hess KR, Mehl RA, Brewer SH (2009) Probing protein folding using site-specifically encoded unnatural amino acids as FRET donors with tryptophan. Biochemistry 48:5953–5962.
84. Rogers JMG, Lippert LG, Gai F (2010) Non-natural amino acid fluorophores for one- and two-step fluorescence resonance energy transfer applications. Anal Biochem 399:182–189.
85. Goldberg JM, Batjargal SPeterson EJ. (2010) Thioamides as fluorescence quenching probes: minimalist chromophores to monitor protein dynamics. J Am Chem Soc 132:14718–14720.
86. Siegel S, Judeikis HS (1968) Relative interaction radii for quenching of triplet-state molecules. J Chem Phys 48:1613–1619.
87. Stone AJ (1997) The theory of intermolecular forces (international series of monographs on chemistry). New York: Oxford University Press Inc.
88. Gonnelli M, Strambini GB (2009) Intramolecular quenching of tryptophan phosphorescence in short peptides and proteins. Photochem Photobio 81:614–622.
89. Lapidus LJ, Eaton WA, Hofrichter J (2000) Measuring the rate of intramolecular contact formation in polypeptides. Proc Natl Acad Sci USA 97:7220–7225.
90. Krieger F, Fierz B, Bieri O, Drewello M, Kiefhaber T (2003) Dynamics of unfolded polypeptide chains as model for the earliest steps in protein folding. J Mol Biol 332:265–274.
91. Huang F, Nau WM (2003) A conformational flexibility scale for amino acids in peptides. Angew Chem Int Ed 42:2269–2272.
92. Reiner A, Henklein P, Kiefhaber T (2010) An unlocking/relocking barrier in conformational fluctuations of villin headpiece subdomain. Proc Natl Acad Sci USA 107:4955–4960.
93. Cellmer T, Buscaglia M, Henry ER, Hofrichter J, Eaton WA (2011) Making connections between ultrafast protein folding kinetics and molecular dynamics simulations. Proc Natl Acad Sci USA 108:6103–6108.
94. Magde D, Elson E, Webb WW (1972) Thermodynamic fluctuations in a reacting system—measurement by fluorescence correlation spectroscopy. Phys Rev Lett 29:705–708.
95. Rigler R, Mets U, Widengren J, Kask P (1993) Fluorescence correlation spectroscopy with high count rate and low-background—analysis of translational diffusion. Eur Biophys J Biophys Lett 22:169–175.
96. Purkayastha P, Klemke J, Lavender S, Oyola R, Cooperman BS, Gai F (2005) α_1-Antitrypsin polymerization: a fluorescence correlation spectroscopic study. Biochemistry 44:2642–2649.
97. Werner JH, Joggerst R, Dyer RB, Goodwin PM (2006) A two-dimensional view of the folding energy landscape of cytochrome c. Proc Natl Acad Sci USA 103: 11130–11135.
98. Chowdhury P, Wang W, Lavender S, Bunagan MR, Klemke JW, Tang J, Saven JG, Cooperman BS, Gai F (2007) Fluorescence correlation spectroscopic study of serpin depolymerization by computationally designed peptides. J Mol Biol 369:462–473.
99. Guo L, Chowdhury P, Glasscock JM, Gai F (2008) Denaturant-induced expansion and compaction of a multi-domain protein: IgG. J Mol Biol 384:1029–1036.
100. Sherman E, Itkin A, Kuttner YY, Rhoades E, Amir D, Haas E, Haran G (2008) Using fluorescence correlation spectroscopy to study conformational changes in denatured proteins. Biophys J 94:4819–4827.
101. Neuweiler H, Johnson CM, Fersht AR (2009) Direct observation of ultrafast folding and denatured state dynamics in single protein molecules. Proc Natl Acad Sci USA 106:18569–18574.
102. Sherman E, Haran G (2011) Fluorescence correlation spectroscopy of fast chain dynamics within denatured protein L. Chemphyschem 12:696–703.
103. Buschmann V, Weston KD, Sauer M (2003) Spectroscopic study and evaluation of red-absorbing fluorescent dyes. Bioconjug Chem 14:195–204.
104. Doose S, Neuweiler H, Sauer M (2005) A close look at fluorescence quenching of organic dyes by tryptophan. Chemphyschem 6:2277–2285.
105. Neuweiler H, Doose S, Sauer M (2005) A microscopic view of miniprotein folding: enhanced folding efficiency through formation of an intermediate. Proc Natl Acad Sci USA 102:16650–16655.
106. Doose S, Neuweiler H, Sauer M (2009) Fluorescence quenching by photoinduced electron transfer: a reporter for conformational dynamics of macromolecules. ChemPhysChem 10:1389–1398.
107. Rogers JMG, Poishchuk AL, Guo L, Wang J, DeGrado WF, Gai F (2011) Photoinduced electron transfer and

fluorophore motion as a probe of the conformational dynamics of membrane proteins: application to the influenza A M2 proton channel. Langmuir 27:3815–3821.
108. Silva RAGD, Yasui SC, Kubelka J, Formaggio F, Crisma M, Toniolo C, Keiderling TA (2002) Discriminating 3_{10}- from α-helices: vibrational and electronic CD and IR absorption study of related aib-containing oligopeptides. Biopolymers 65:229–243.
109. Kennedy DF, Crisma M, Toniolo C, Chapman D (1991) Studies of peptides forming 3_{10}-helices and α-helices and β-bend ribbon structures in organic solution and in model biomembranes by Fourier-transform infrared-spectroscopy. Biochemistry 30:6541–6548.
110. Reinstadler D, Fabian H, Backmann J, Naumann D (1996) Refolding of thermally and urea-denatured ribonuclease A monitored by time-resolved FTIR spectroscopy. Biochemistry 35:15822–15830.
111. From NB, Bowler BE (1998) Urea denaturation of staphylococcal nuclease monitored by Fourier transform infrared spectroscopy. Biochemistry 37:1623–1631.
112. Goormaghtigh E, Raussens V, Ruysschaert JM. (1999) Attenuated total reflection infrared spectroscopy of proteins and lipids in biological membranes. Biochim Biophys Acta Rev Biomembr 1422:105–185.
113. Silva RAGD, Kubelka J, Bour P, Decatur SM, Keiderling TA (2000) Site-specific conformational determination in thermal unfolding studies of helical peptides using vibrational circular dichroism with isotopic substitution. Proc Natl Acad Sci USA 97:8318–8323.
114. Barth A, Zscherp C (2002) What vibrations tell us about proteins. Q Rev Biophys 35:369–430.
115. Keiderling TA (2002) Protein and peptide secondary structure and conformational determination with vibrational circular dichroism. Curr Opin Chem Biol 6:682–688.
116. Mukherjee S, Chowdhury P, Gai F (2006) Tuning the cooperativity of the helix–coil transition by aqueous reverse micelles. J Phys Chem B 110:11615–11619.
117. Miyazawa T (1960) Perturbation treatment of the characteristic vibrations of polypeptide chains in various configurations. J Chem Phys 32:1647–1652.
118. Krimm S, Bandekar J (1986) Vibrational spectroscopy and conformation of peptides, polypeptides, and proteins. Adv Protein Chem 38:181–364.
119. Hamm P, Lim M, DeGrado WF, Hochstrasser RM (1999) The two-dimensional IR nonlinear spectroscopy of a cyclic penta-peptide in relation to its three-dimensional structure. Proc Natl Acad Sci USA 96:2036–2041.
120. Mukamel S, Abramavicius D (2004) Many-body approaches for simulating coherent nonlinear spectroscopies of electronic and vibrational excitons. Chem Rev 104:2073–2098.
121. Montalvo G, Waegele MM, Shandler S, Gai F, DeGrado WF (2010) Infrared signature and folding dynamics of a helical β-peptide. J Am Chem Soc 132:5616–5618.
122. Mukherjee S, Chowdhury P, Gai F (2007) Infrared study of the effect of hydration on the amide I band and aggregation properties of helical peptides. J Phys Chem B 111:4596–4602.
123. Huang CY, Getahun Z, Zhu YJ, Klemke JW, DeGrado WF, Gai F (2002) Helix formation via conformation diffusion search. Proc Natl Acad Sci USA 99: 2788–2793.
124. Xu Y, Oyola R, Gai F (2003) Infrared study of the stability and folding kinetics of a 15-residue β-hairpin. J Am Chem Soc 125:15388–15394.
125. Bunagan MR, Gao J, Kelly JW, Gai F (2009) Probing the folding transition state structure of the villin headpiece subdomain via side chain and backbone mutagenesis. J Am Chem Soc 131:7470–7476.
126. Bunagan MR, Yang X, Saven JG, Gai F (2006) Ultrafast folding of a computationally designed trp-cage mutant: Trp^2-cage. J Phys Chem B 110:3759–3763.
127. Culik RM, Serrano AL, Bunagan MR, Gai F (2011) Achieving secondary structural resolution in kinetic measurements of protein folding: a case study of the folding mechanism of trp-cage. Angew Chem Int Ed 50:10884–10887.
128. Du D, Zhu YJ, Huang CY, Gai F (2004) Understanding the key factors that control the rate of β-hairpin folding. Proc Natl Acad Sci USA 101:15915–15920.
129. Du D, Tucker MJ, Gai F. (2006) Understanding the mechanism of β-hairpin folding via phi-value analysis. Biochemistry 45:2668–2678.
130. Xu Y, Wang T, Gai F (2006) Strange temperature dependence of the folding rate of a 16-residue β-hairpin. Chem Phys 323:21–27.
131. Du D, Gai F (2006) Understanding the folding mechanism of an alpha-helical hairpin. Biochemistry 45: 13131–13139.
132. Waegele MM, Gai F (2010) Infrared study of the folding mechanism of a helical hairpin: porcine PYY. Biochemistry 49:7659–7664.
133. Neidigh JW, Fesinmeyer RM, Andersen NH (2002) Designing a 20-residue protein. Nat Struct Biol 9: 425–430.
134. Barua B, Lin JC, Williams VD, Kummler P, Neidigh JW, Andersen NH (2008) The trp-cage: optimizing the stability of a globular miniprotein. Protein Eng Des Sel 21:171–185.
135. Wilson EB, Decius JC, Cross PC (1980) Molecular vibrations: the theory of infrared and Raman vibrational spectra. New York: Dover.
136. Mirkin NG, Krimm S (1996) Ab initio vibrational analysis of isotopic derivatives of aqueous hydrogen-bonded trans-N-methylacetamide. J Mol Struct 377:219–234.
137. Decatur SM, Antonic J (1999) Isotope-edited infrared spectroscopy of helical peptides. J Am Chem Soc 121: 11914–11915.
138. Brauner JW, Dugan C, Mendelsohn R (2000) C-13 isotope labeling of hydrophobic peptides. Origin of the anomalous intensity distribution in the infrared amide I spectral region of β-sheet structures. J Am Chem Soc 122:677–683.
139. Huang CY, Getahun Z, Wang T, DeGrado WF, Gai F (2001) Time-resolved infrared study of the helix–coil transition using C-13-labeled helical peptides. J Am Chem Soc 123:12111–12112.
140. Waegele MM, Culik RM, Gai F (2011) Site-specific spectroscopic reporters of the local electric field, hydration, structure, and dynamics of biomolecules. J Phys Chem Lett 2:2598–2609.
141. Wang Y, Purrello R, Jordan T, Spiro TG (1991) UVRR spectroscopy of the peptide-bond. 1. Amide-S, a non-helical structure marker, is a C_α—H bending mode. J Am Chem Soc 113:6359–6368.
142. Wang Y, Purrello R, Georgiou S, Spiro TG (1991) UVRR spectroscopy of the peptide-bond. 2. Carbonyl H-bond effects on the ground-state and excited-state structures of N-methylacetamide. J Am Chem Soc 113:6368–6377.
143. Huang CY, Balakrishnan G, Spiro TG (2006) Protein secondary structure from deep-UV resonance Raman spectroscopy. J Raman Spectrosc 37:277–282.
144. Chi Z, Chen XG, Holtz JSW, Asher SA (1998) UV resonance Raman-selective amide vibrational enhancement: quantitative methodology for determining protein secondary structure. Biochemistry 37:2854–2864.
145. Oladepo SA, Xiong K, Hong Z, Asher SA (2011) Elucidating peptide and protein structure and dynamics:

UV resonance Raman spectroscopy. J Phys Chem Lett 2:334–344.
146. Asher SA, Ianoul A, Mix G, Boyden MN, Karnoup A, Diem M, Schweitzer-Stenner R. (2001) Dihedral psi angle dependence of the amide III vibration: a uniquely sensitive UV resonance Raman secondary structural probe. J Am Chem Soc 123:11775–11781.
147. Lednev IK, Karnoup AS, Sparrow MC, Asher SA (1999) α-Helix peptide folding and unfolding activation barriers: a nanosecond UV resonance Raman study. J Am Chem Soc 121:8074–8086.
148. Lednev IK, Karnoup AS, Sparrow MC, Asher SA (2001) Transient UV Raman spectroscopy finds no crossing barrier between the peptide α-helix and fully random coil conformation. J Am Chem Soc 123:2388–2392.
149. Mikhonin AV, Asher SA (2005) Uncoupled peptide bond vibrations in α-helical and polyproline II conformations of polyalanine peptides. J Phys Chem B 109:3047–3052.
150. Huang CY, Balakrishnan G, Spiro TG (2005) Early events in apomyoglobin unfolding probed by laser T-jump/UV resonance Raman spectroscopy. Biochemistry 44:15734–15742.
151. JiJi RD, Balakrishnan G, Hu Y, Spiro TG (2006) Intermediacy of poly(L-proline) II and β-strand conformations in poly(L-lysine) β-sheet formation probed by temperature-jump/UV resonance Raman spectroscopy. Biochemistry 45:34–41.
152. Zanni MT, Gnanakaran S, Stenger J, Hochstrasser RM (2001) Heterodyned two-dimensional infrared spectroscopy of solvent-dependent conformations of acetylproline-NH_2. J Phys Chem B 105:6520–6535.
153. Gnanakaran S, Hochstrasser RM (2001) Conformational preferences and vibrational frequency distributions of short peptides in relation to multidimensional infrared spectroscopy. J Am Chem Soc 123:12886–12898.
154. Remorino A, Korendovych IV, Wu Y, DeGrado WF, Hochstrasser RM (2011) Residue-specific vibrational echoes yield 3D structures of a transmembrane helix dimer. Science 332:1206–1209.
155. Kim YS, Hochstrasser RM (2009) Applications of 2D IR spectroscopy to peptides, proteins, and hydrogen-bond dynamics. J Phys Chem B 113:8231–8251.
156. Hochstrasser RM (2007) Two-dimensional spectroscopy at infrared and optical frequencies. Proc Natl Acad Sci USA 104:14190–14196.
157. Zhuang W, Sgourakis NG, Li Z, Garcia AE, Mukamel S (2010) Discriminating early stage A β 42 monomer structures using chirality-induced 2DIR spectroscopy in a simulation study. Proc Natl Acad Sci USA 107:15687–15692.
158. Ganim Z, Chung HS, Smith AW, Deflores LP, Jones KC, Tokmakoff A (2008) Amide I two-dimensional infrared spectroscopy of proteins. Acc Chem Res 41:432–441.
159. Moran AM, Park SM, Dreyer J, Mukamel S (2003) Linear and nonlinear infrared signatures of local α- and 3_{10}-helical structures in alanine polypeptides. J Chem Phys 118:3651–3659.
160. Urbanek DC, Vorobyev DY, Serrano AL, Gai F, Hochstrasser RM (2010) The two-dimensional vibrational echo of a nitrile probe of the villin HP35 protein. J Phys Chem Lett 1:3311–3315.
161. Maekawa H, Toniolo C, Moretto A, Broxterman QB, Ge NH (2006) Different spectral signatures of octapeptide 3_{10}- and α-helices revealed by two-dimensional infrared spectroscopy. J Phys Chem B 110:5834–5837.
162. Sul S, Karaiskaj D, Jiang Y, Ge NH. (2006) Conformations of N-acetyl-L-prolinamide by two-dimensional infrared spectroscopy. J Phys Chem B 110:19891–19905.
163. Zhuang W, Hayashi T, Mukamel S (2009) Coherent multidimensional vibrational spectroscopy of biomolecules: concepts, simulations, and challenges. Angew Chem Int Edit 48:3750–3781.
164. Maekawa H, De Poli M, Moretto A, Toniolo C, Ge N (2009) Toward detecting the formation of a single helical turn by 2D IR cross peaks between the Amide-I and -II modes. J Phys Chem B 113:11775–11786.
165. Jeon J, Yang S, Choi J, Cho M (2009) Computational vibrational spectroscopy of peptides and proteins in one and two dimensions. Acc Chem Res 42:1280–1289.
166. Chung HS, Khalil M, Smith AW, Tokmakoff A (2007) Transient two-dimensional IR spectrometer for probing nanosecond temperature-jump kinetics. Rev Sci Instrum 78:063101.
167. Smith AW, Tokmakoff A (2007) Probing local structural events in β-hairpin unfolding with transient nonlinear infrared spectroscopy. Angew Chem Int Edit 46:7984–7987.
168. Smith AW, Lessing J, Ganim Z, Peng CS, Tokmakoff A, Roy S, Jansen TLC, Knoester J (2010) Melting of a β-hairpin peptide using isotope-edited 2D IR spectroscopy and simulations. J Phys Chem B 114: 10913–10924.
169. Shim SH, Strasfeld DB, Ling YL, Zanni MT (2007) Automated 2D IR spectroscopy using a mid-IR pulse shaper and application of this technology to the human islet amyloid polypeptide. Proc Natl Acad Sci USA 104:14197–202.
170. Mukherjee S, Chowdhury P, Gai F (2009) Effect of dehydration on the aggregation kinetics of two amyloid peptides. J Phys Chem B 113:531–535.
171. Shim SH, Gupta R, Ling YL, Strasfeld DB, Raleigh DP, Zanni MT (2009) Two-dimensional IR spectroscopy and isotope labeling defines the pathway of amyloid formation with residue-specific resolution. Proc Natl Acad Sci USA 106:6614–6619.
172. Kim YS, Liu L, Axelsen PH, Hochstrasser RM (2009) 2D IR provides evidence for mobile water molecules in β-amyloid fibrils. Proc Natl Acad Sci USA 106: 17751–17756.
173. Londergan CH, Wang J, Axelsen PH, Hochstrasser RM (2006) Two-dimensional infrared spectroscopy displays signatures of structural ordering in peptide aggregates. Biophys J 90:4672–4685.
174. Mukherjee P, Kass I, Arkin IT, Zanni MT (2006) Picosecond dynamics of a membrane protein revealed by 2D IR. Proc Natl Acad Sci USA 103:3528–3533.
175. Guo L, Chowdhury P, Fang JY, Gai F (2007) Heterogeneous and anomalous diffusion inside lipid tubules. J Phys Chem B 111:14244–1429.
176. Guo L, Gai F (2010) Heterogeneous diffusion of a membrane-bound pHLIP peptide. Biophys J 98:2914–2922.
177. Smith-Dupont KB, Guo L, Gai F (2010) Diffusion as a probe of the heterogeneity of antimicrobial peptide-membrane interactions. Biochemistry 49:4672–468.
178. Ghosh A, Qiu J, DeGrado WF, Hochstrasser RM (2011) Tidal surge in the M2 proton channel, sensed by 2D IR spectroscopy. Proc Natl Acad Sci USA 108:6115–6120.
179. Ansari A, Kuznetsov SV (2005) Is hairpin formation in single-stranded polynucleotide diffusion-controlled? J Phys Chem B 109:12982–12989.
180. Brauns EB, Dyer RB (2005) Time-resolved infrared spectroscopy of RNA folding. Biophys J 89:3523–3530.
181. Ma H, Proctor DJ, Kierzek E, Kierzek R, Bevilacqua PC, Gruebele M (2006) Exploring the energy landscape of a small RNA hairpin. J Am Chem Soc 128:1523–1530.
182. Kuznetsov SV, Sugimura S, Vivas P, Crothers DM, Ansari A (2006) Direct observation of DNA bending/unbending kinetics in complex with DNA-bending protein IHF. Proc Natl Acad Sci USA 103:18515–18520.